Correlating Structure and Affinity for PEX5:PTS1 Complexes †

ARTICLE *in* BIOCHEMISTRY · MARCH 2003

Impact Factor: 3.02 · DOI: 10.1021/bi027034z · Source: PubMed

6 AUTHORS, INCLUDING:

Ernest L. Maynard
Novavax
22 PUBLICATIONS **405** CITATIONS
SEE PROFILE

Brian Geisbrecht
Kansas State University
74 PUBLICATIONS **2,036** CITATIONS
SEE PROFILE

Correlating Structure and Affinity for PEX5:PTS1 Complexes†

Gregory J. Gatto, Jr.,‡ Ernest L. Maynard,‡ Anthony L. Guerrerio,‡ Brian V. Geisbrecht,§ Stephen J. Gould,§ and Jeremy M. Berg*,‡

Department of Biophysics and Biophysical Chemistry and Department of Biological Chemistry, Johns Hopkins University School of Medicine, Baltimore, Maryland 21205

Received October 18, 2002; Revised Manuscript Received December 10, 2002

ABSTRACT: Many proteins that are destined to reside within the lumen of the peroxisome contain the peroxisomal targeting signal-1 (PTS1), a C-terminal tripeptide approximating the consensus sequence −Ser−Lys−Leu−COO^-. The PTS1 is recognized by the tetratricopeptide repeat (TPR) domains of PEX5, a cytosolic receptor that cycles between the cytoplasm and the peroxisome. To gain insight into the energetics of PTS1 binding specificity and to correlate these with features from the recently determined structure of a PEX5:PTS1 complex, we used a fluorescence-based binding assay that enables the quantitation of the dissociation constants for PTS1-containing peptide complexes with the TPR region of human PEX5. Through application of this assay to a collection of pentapeptides containing different C-terminal tripeptide sequences, including both natural and unnatural amino acids, the thermodynamic effects of sequence variation were examined. PTS1 variants that correspond to known functional targeting signals bind to the PEX5 fragment with a change in the standard binding free energy within 1.8 kcal mol^{-1} of that corresponding to the peptide ending with −Ser−Lys−Leu−COO^-. The results suggest that a binding energy threshold may determine the functionality of PTS1 sequences.

Peroxisomes are membrane-bound organelles that participate in a number of cellular metabolic processes, including the β-oxidation of certain fatty acids and the biosynthesis of cholesterol, bile acids, and plasmalogens (*1*). Failure to properly assemble peroxisomes in humans leads to a group of genetic disorders known as the peroxisome biogenesis disorders (PBDs)[1], which include the Zellweger spectrum−Zellweger syndrome, neonatal adrenoleukodystrophy, and infantile Refsum disease—and rhizomelic chondrodysplasia punctata (*2*, *3*). These PBDs result from mutations in any one of a group of genes that encode peroxins, proteins specifically involved in peroxisomal protein targeting and import.

Proteins that reside within the lumen, or matrix, of the peroxisome are first completely synthesized by ribosomes in the cytosol. Most peroxisomal matrix proteins contain the peroxisomal targeting signal-1 (PTS1), a C-terminal tripeptide sufficient to achieve correct subcellular localization (*4*). The receptor for the PTS1, PEX5, cycles between the cytosol and the peroxisome, where import into the organelle occurs (*5*, *6*). PEX5 recognizes the PTS1 using six tetratricopeptide repeat motifs (TPRs) located within its C-terminal half (*5*, *7*, *8*). We have recently reported the crystal structure of a fragment of human PEX5 containing the entire TPR array (PEX5-C) complexed with a pentapeptide containing a canonical PTS1 sequence (*8*). Backbone atoms from the PTS1 are bound by a collection of asparagine residues from within the receptor, while the side chain atoms and the terminal carboxylate of the PTS1 are recognized by a series of pockets that confer sequence specificity.

While the PTS1 is typically described by its consensus sequence, −Ser−Lys−Leu−COO^-, it has been demonstrated that conservative substitutions within this tripeptide do yield functional targeting signals. For example, in mammalian cells, Ala and Cys are allowed at the -3 position, His and Arg at the -2 position, and Met at the -1 position (*4*, *9*). Subsequent studies have attempted to further explore these requirements. For example, Elgersma et al. used random mutagenesis of the PTS1 from *Saccharomyces cerevisiae* malate dehydrogenase to generate a library of possible C-terminal tripeptides (*10*). Functional assessment of these tripeptides involved the comparison of a Western blot of the organellar pellet versus the cytosolic supernatant. In addition, Hartig and co-workers (*11*) used a yeast two-hybrid assay in which human and *S. cerevisiae* PEX5 were screened against a random peptide library, and the strength of the interaction was measured using β-galactosidase reporter expression. Additional experiments have been performed to explore the PTS1 requirements for glycosomal import in trypanosomes and glyoxysomal/peroxisomal import in plants (*12*−*14*). The results from all these studies suggest that there may be more variation allowed within the PTS1 than originally anticipated and that there are species-specific differences between the tripeptide sequence families recognized by PEX5. However, the lack of precision of the assays precludes a more detailed analysis.

† Supported by NIH Grant P01GM51362 to J.M.B., NIH Grant F32DK060371 to E.L.M., and the NIH Medical Scientist Training Program to G.J.G. and A.L.G.

* To whom correspondence should be addressed. Phone: (410) 955-8712. Fax: (410) 502-6910. E-mail: jberg@jhmi.edu.

‡ Department of Biophysics and Biophysical Chemistry.

§ Department of Biological Chemistry.

[1] Abbreviations: PTS1, peroxisomal targeting signal-1; TPR, tetratricopeptide repeat; PBD, peroxisome biogenesis disorder; Hnl, 6-hydroxynorleucine; Hse, homoserine; Fmoc, 9-fluorenylmethoxycarbonyl; HOBt, 1-hydroxybenzotriazole; TBTU, *O*-(benzotriazol-1-yl)-*N*,*N*, *N*′,*N*′-tetramethyluronium tetrafluoroborate.

10.1021/bi027034z CCC: $25.00
Published on Web 01/24/2003

In our report of the crystal structure of the PEX5-C:PTS1 complex, we used a binding assay to confirm the functional activity of the PEX5 fragment as well as test the activity of a form of PEX5-C that carried a mutation known to cause disease in humans (*8*). These experiments were based on changes in fluorescence anisotropy of a lissamine-tagged peptide upon addition of receptor protein. In the work presented here, this assay is expanded to determine the affinities of unlabeled peptides for PEX5-C by measuring their ability to displace labeled ligand, facilitating examination of an extensive series of peptides.

EXPERIMENTAL PROCEDURES

Protein Expression and Purification. PEX5-C, a 41 kDa fragment of human PEX5 comprised of amino acids 235−602, was expressed and purified as previously described (*8*).

Peptide Synthesis. All peptides were synthesized by solid-phase methods on a MilliGen/Biosearch 9050 Peptide Synthesizer using 9-fluorenylmethoxycarbonyl (Fmoc) chemistry with *O*-(benzotriazol-1-yl)-*N*,*N*,*N*′,*N*′-tetramethyluronium tetrafluoroborate (TBTU) and 1-hydroxybenzotriazole (HOBt) activation. The unnatural amino acids homoserine (Hse) and 6-hydroxynorleucine (Hnl) were purchased in a side chain-protected form appropriate for solid-phase peptide synthesis from Novabiochem and Advanced ChemTech, respectively. The peptide amide, YQSKL−$CONH_2$, was synthesized on the NovaSyn TGR resin (Novabiochem). All peptides contained a tyrosine residue at the -5 position to enable quantitation by UV/vis spectrophotometry (ϵ_{274} = 1400 M^{-1} cm^{-1}). Peptides that contained cysteine were prepared in degassed water and stored in an anaerobic environment to prevent side chain oxidation. Peptide identity and purity was confirmed by MALDI/TOF mass spectrometry. Labeled YQSKL was prepared by conjugation of the rhodamine derivative lissamine to the N-terminus of the peptide via a sulfonamide linkage (Figure 1A), as previously described (*8*, *15*).

Fluorescence Anisotropy Titrations. We have noted during these experiments that both the fluorescent peptide and the protein fragment have the propensity to adhere to cuvette walls, yielding fluorescence intensity and anisotropy signals inconsistent both within a given titration and from one experiment to the next. Successful inhibition of these processes was achieved by pretreatment of the cuvettes with gelatin. A total of 40 μL of a 20 mg mL^{-1} solution of 175 Bloom porcine gelatin (Sigma) was added to 2.5 mL of 100 mM NaCl and 10 mM HEPES (pH 7.5) in a 3.5 mL Spectrosil Far UV Quartz window fluorescence cuvette (Starna Cells, Inc.) equipped with a magnetic stirring bar. The cuvette was maintained at 25 °C with continuous stirring for the next 12 h. Lissamine−YQSKL was then added to a final concentration of 200 nM. Before introduction of any additional reagents, the stability of the fluorescence signal was confirmed by measuring emission spectra over the next 1−2 h. PEX5-C was then added to a final concentration of 500 nM. All fluorescence anisotropy measurements were made on a Horiba Jobin Yvon Spex Fluorolog-3 fluorometer equipped with excitation and emission polarizers, configured in the L-format. The excitation monochromator was set to a wavelength of 568 nm with a slit width of 2 nm, and the emission monochromator was set to a wavelength of 588 nm with a slit width of 4 nm. Each measurement was made with a 5 s integration time. At each titration point, measurements were obtained in triplicate with at least 10 min between each reading to confirm signal stability. In all experiments, the sample cell was maintained at a constant temperature of 25 °C using a Neslab RTE-111 bath circulator.

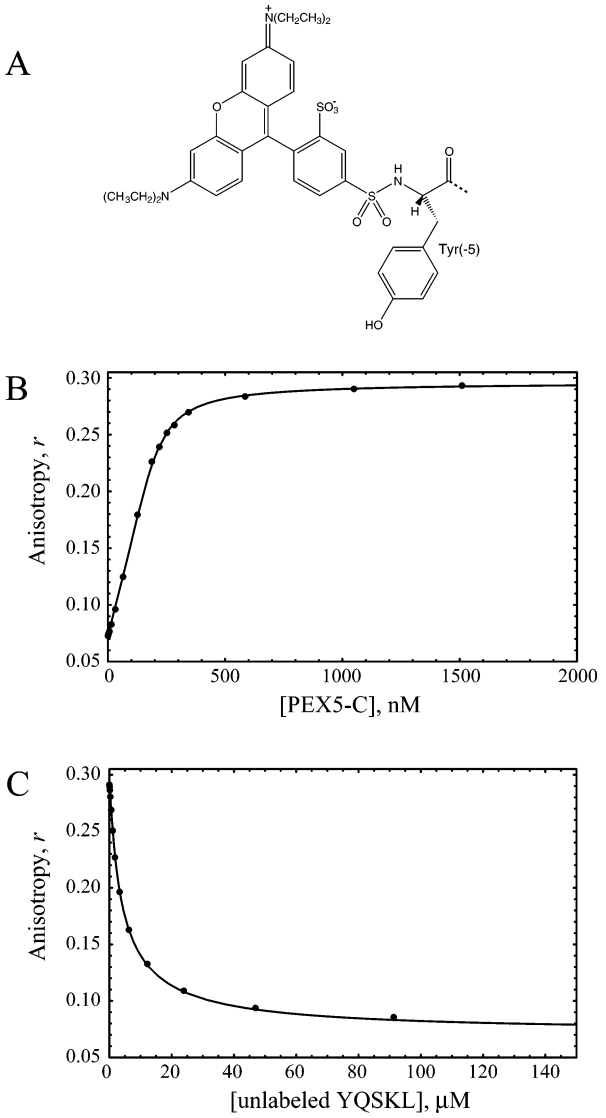

FIGURE 1: Examples of fitted titration results using lissamine-conjugated YQSKL. (A) Structure of the rhodamine derivative lissamine covalently attached to the peptide N-terminus through a sulfonamide linkage. Only the first residue of the peptide, Tyr (-5), is shown. (B) Titration of PEX5-C into 200 nM lissamine−YQSKL. (C) Competition titration of unlabeled YQSKL into 200 nM lissamine−YQSKL and 500 nM PEX5-C.

Data Analysis. Determination of the fraction of fluorophore bound (f_B) for a given anisotropy value (r) is computed with the expression

$$f_B = \frac{r - r_{free}}{r_{bound} - r_{free}}$$

given the anisotropy of the free (r_{free}) and bound (r_{bound}) fluorophore. This expression must be modified if there are changes in the fluorescence intensity during the binding event. In this case, a correction factor, Q, representing the

quantum yield ratio of the bound to the free form, must be introduced

$$f_B = \frac{r - r_{free}}{(r_{bound} - r)Q + (r - r_{free})}$$

Typically, Q can be estimated by the ratio of the intensities of the bound to the free species. Prior to all curve-fitting in these experiments, this correction was applied since a decrease in the fluorescence intensity was consistently observed upon ligand binding ($Q = 0.64$). For the simple forward titrations of protein into lissamine−YQSKL, the data were fit using Kaleidagraph (Synergy Software). For the competition titrations, a curve-fitting algorithm in Mathematica (Wolfram Research) was applied to all data for each experiment. This algorithm searches through a range of dissociation constants for complex of the unlabeled peptide for the receptor and finds the best fit to the observed data, given estimates for the total amount of fluorescent ligand, the total amount of protein, and the dissociation constant for the complex of the labeled peptide.

RESULTS

Assay Design. Fluorescence anisotropy is a measure of the difference in parallel versus perpendicular light emission after excitation of a fluorophore with polarized light (*16*, *17*). Essentially, it represents the tumbling rate of the fluorophore: if the fluorophore is unbound, it will tumble rapidly, and the anisotropy will be low; if large or bound by a much larger molecule, the fluorophore will tumble slowly, and the resulting anisotropy will be high. In the experiments presented here, the fluorophore is a lissamine moiety conjugated to the N-terminus of the pentapeptide YQSKL. Measurement of affinity of a ligand for its receptor can be achieved by titrating receptor into a cuvette containing labeled ligand and detecting the concomitant increase in fluorescence anisotropy (Figure 1B). This type of experiment is simple to perform and generates data that are easily analyzed. However, several disadvantages are present: the experiment consumes considerable protein for each titration and requires the syntheses of many different fluorescent ligands. Furthermore, this design yields a dissociation constant for the peptide with the fluorophore attached, which may be disadvantageous if the dye moiety alters binding.

To overcome these drawbacks, we performed a series of competition experiments in which the receptor protein is first added to the labeled ligand at a level near saturation, then a second unlabeled ligand is titrated, and the decay of signal is observed. Such an experiment requires less protein, necessitates the synthesis of only one fluorescent ligand, and enables the measurement of the affinity of the unlabeled ligand, thus eliminating any effects of the fluorophore. Hence, this design is ideal for determining the affinities for a group of competitor peptides. The only significant disadvantage of the competition assay is that more complex data analysis methods are required.

An example of the competition experiment is shown in Figure 1C, in which unlabeled YQSKL served as the competitor. Optimal agreement between the observed and the calculated binding curves was obtained with the use of the following values: $K_1 = 15$ nM and $K_2 = 190$ nM, where K_1 and K_2 are the dissociation constants for the lissamine−YQSKL peptide and the unlabeled YQSKL peptide, respectively. The decrease in binding affinity upon removal of the lissamine modification at the N-terminus suggests that this group significantly interacts with PEX5-C, consistent with the fluorescence intensity change and substantial anisotropy increase observed upon binding.

Affinities of Variant PTS1-Containing Peptides. To probe the sequence requirements of the PTS1, a family of peptides were synthesized, each carrying a single mutation within its C-terminal three amino acids. Competition titrations of each of the peptides with PEX5-C were performed, and the data were analyzed to derive the best-fit dissociation constants. The corresponding changes in standard binding free energy ($\Delta\Delta G°$) relative to YQSKL are presented in Figure 2.

In the crystal structure of the PEX5-C:PTS1 complex, the side chain of the leucine residue at position -1 lies in a hydrophobic pocket defined by residues Val 374, Thr 377, Lys 490, and Ala 493 (Figure 3A). To determine the variability allowed at the -1 position of the PTS1, the following peptides were used: YQSKM, YQSKF, YQSKI, and YQSKA (Figure 3B). Methionine at the -1 position has been previously observed as functional in humans (*9*). This substitution resulted in a 11-fold loss in affinity. A phenylalanine mutation at the -1 position, shown to render the PTS1 nonfunctional in humans (*4*) although still functional in *S. cerevisiae* (*10*) and plants (*13*), yielded an 78-fold reduction in binding. Similarly, mutation of the -1 position to isoleucine has been shown to render the PTS1 nonfunctional in humans (*4*). However, SKI appears to be functional in plants, as determined by Mullen et al. (*13*). A pentapeptide carrying this isoleucine mutation (YQSKI) behaved similarly to YQSKF, with a 48-fold reduction in affinity relative to YQSKL. Mutation of the -1 residue to alanine resulted in a dramatic reduction in affinity of nearly 3 orders of magnitude.

The lysine side chain in position -2 lies in a relatively large, negatively charged pocket with residues primarily from TPR motifs 1−3 of PEX5 (Figure 3C). No direct contacts with the ammonium group of the lysine side chain are observed, but water mediated contacts are present. To test variability at this position, the following peptides were used: YQSRL, YQSHL, YQSNL, YQSEL, and YQSAL (Figure 3D). Of these, arginine and histidine were previously determined to be functional, while a glutamate substitution resulted in a nonfunctional signal (*4*). Arginine at the -2 position yielded only a 1.7-fold loss in affinity, suggesting that this residue is well-accommodated by the negatively charged pocket in PEX5. Mutation at this position to histidine resulted in a 8.5-fold decrease in binding. The rank order of the relative affinities for these three variants (K_d: SKL < SRL < SHL) corresponds well with the hierarchy of targeting efficiencies of these sequences as determined by Swinkels et al. (*9*) Asparagine at the -2 position yields a considerable reduction in binding (28-fold increase in K_d), while mutation to alanine dramatically reduced the affinity for PEX5-C by 150-fold. Binding of the pentapeptide YQSEL to PEX5-C was undetectable, underscoring the importance of the charge on the residue at this position. More detailed analysis of the electrostatic contribution to this binding specificity is presented below.

The serine residue in position -3 is buried relatively deeply in a small pocket in PEX5 (Figure 3E). The serine hydroxyl

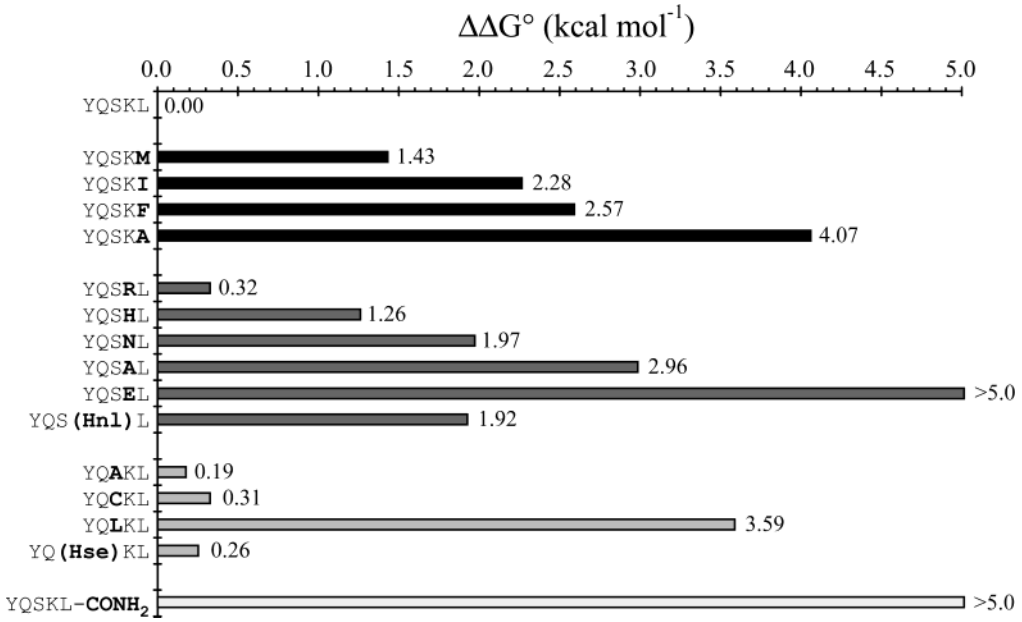

FIGURE 2: Effects of single point mutations on the binding of PTS1-containing pentapeptides to PEX5-C. Affinities are expressed as the change in the free energy of the association reaction ($\Delta\Delta G°$), expressed in kcal mol^{-1}, relative to the pentapeptide containing YQSKL. The errors in these free energy values are estimated to be 0.2 kcal mol^{-1}.

group is hydrogen bonded to a water molecule that is likely to be tightly bound by the protein, based on extensive contacts with conserved structural features. Peptides containing variations at the -3 position tested using this assay included YQCKL, YQAKL, and YQLKL. The titrations for these peptides are shown in Figure 3F. The best-fit dissociation constants for these peptides indicate that small amino acids at position -3 known to result in functional targeting signals are tolerated well. Both YQAKL and YQCKL bind to PEX5-C with an affinity within approximately 2-fold of that of YQSKL. As with the functional variants at the -2 position, the rank order of the relative affinities for these peptides (K_d: SKL < AKL < CKL) correlates well with the functional hierarchy determined previously (*9*). Mutation at this position to the much larger leucine residue, however, results in a severe impairment of peptide recognition by nearly 3 orders of magnitude worse than YQSKL, consistent with the highly constrained binding pocket.

Use of Unnatural Amino Acids to Probe the PEX5:PTS1 Interaction. One of the advantages of the competition assay is that it enables the affinity measurement for PEX5 of a wide variety of molecules. For instance, nonpeptide small molecules, cyclic peptides, and whole proteins can be tested for their affinity to the PTS1 recognition site of PEX5 without the need for labeling. In addition, unnatural amino acids can be incorporated into the competitor peptide, allowing for the opportunity to probe the PEX5:PTS1 interaction in a highly directed fashion.

Two of the three side chain binding pockets have been explored with unnatural amino acids. First, a peptide containing 6-hydroxynorleucine (Hnl) at position -2 was tested. This side chain has the same structure as lysine, except the amino group has been replaced by a hydroxyl group (Figure 4A). Hence, it has similar overall features as lysine in terms of hydrogen bonding and side chain geometry except the positive charge has been removed. This peptide, YQS(Hnl)L, binds to PEX5-C approximately 26-fold less tightly relative to YQSKL, a net impact of nearly 2 kcal mol^{-1} on the binding standard free energy because of charge removal (Figures 2 and 4B).

Second, the serine binding pocket was probed in a similar manner. As discussed above, the PEX5-C:PTS1 crystal structure revealed that the Ser (-3) from the peptide ligand contacts the receptor through a single intervening water molecule (Figure 3E). The unnatural amino acid homoserine has an additional methylene group, extending the side chain so that its hydroxyl group might be expected to project further into this pocket and perhaps displace the water molecule normally bound to PEX5 with favorable entropic consequences (Figure 5A). Competition titration of YQ(Hse)KL yielded a 1.5-fold loss in affinity as compared with the parent YQSKL peptide (Figures 2 and 5B). While this molecule did not bind to PEX5-C more tightly than the wild-type peptide, it is encouraging that the side chain in the -3 position could be made larger without a significant loss of affinity. In fact, this homoserine-containing peptide bound PEX5-C more tightly than YQCKL, a known functional PTS1 in vivo (*4*). This observation suggests, but does not prove, that the proposed binding mode has been achieved.

Last, the terminal carboxylate binding pocket was also studied using this approach. In the crystal structure, the C-terminus of the PTS1 is recognized by both direct and water-mediated contacts from Asn 378, Asn 489, Lys 490, and Arg 520. This interaction was probed using a peptide containing a neutral terminal amide, YQSKL−$CONH_2$. Titration of this peptide as competitor yielded no observable binding (Figure 2), confirming the importance of the free carboxylate within this pocket.

DISCUSSION

It has been well established that significant variability is permitted within PTS1 sequences. What, then, determines if a particular tripeptide will function as a targeting signal? One possible mechanism suggests that there is a threshold affinity of the peptide for the TPR domains of PEX5. If its

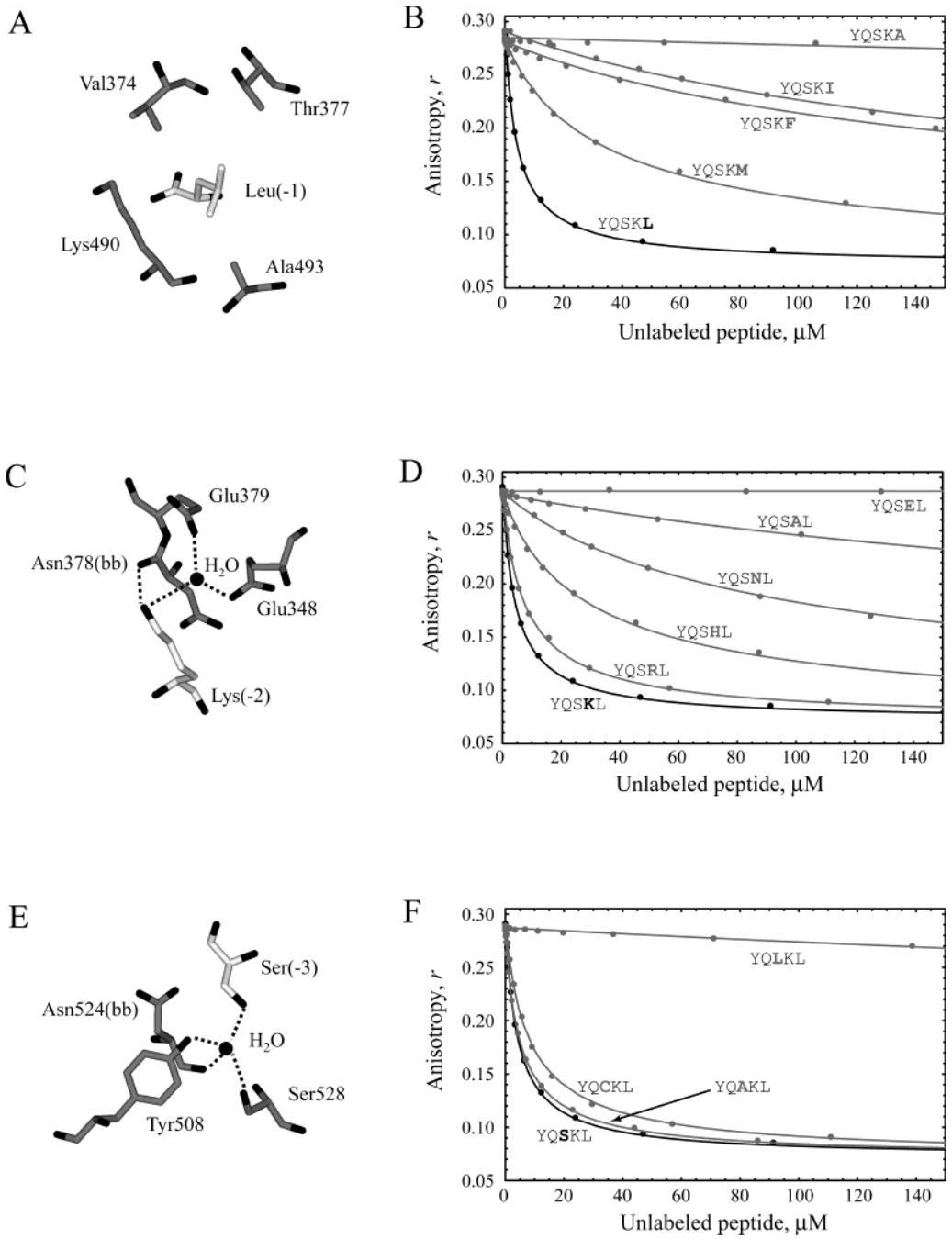

FIGURE 3: Results of competition experiments. Titration points are shown for pentapeptides varying by single mutations at each of the three positions of the PTS1. Curves were generated using the data fitting algorithm in Mathematica. Views of the binding pockets in panels A, C, and E are from the PEX5-C:PTS1 crystal structure, with residues from the PTS1 peptide in white and those from the receptor in gray (nitrogen and oxygen atoms are in black). The results for YQSKL in panels B, D, and F are shown in black. (A) Leu (-1) binding pocket. (B) Titration results for -1 position mutants. (C) Lys (-2) binding pocket. (D) Titration results for -2 position mutants. (E) Ser (-3) binding pocket. (F) Titration results for -3 position mutants. Molecular representations in panels A, C, and E were constructed using MOLSCRIPT (*24*).

affinity for the receptor is tighter than this threshold, a given sequence will function as a peroxisomal targeting signal. To define this possible threshold, the data generated from varying the -1 position (Figure 3A) is particularly informative. These results cover a wide range of affinities for sequences that have been studied within a common sequence context in mammalian cells. Both leucine and methionine (*4*, *9*) are functional at the -1 position of the PTS1 in humans, but phenylalanine and isoleucine are not (*4*). Hence, the threshold affinity in humans appears to reside in the range between those for YQSKI and YQSKM, corresponding to a $\Delta\Delta G°$ within 1.8 kcal mol^{-1} relative to YQSKL. The $\Delta\Delta G°$ values of the other peptides used in this study with C-terminal sequences known to be functional in vivo—YQAKL, YQCKL, YQSRL, and YQSHL—are all consistent with this threshold.

Ascribing an absolute K_d value for this threshold is not possible at present. This study uses short peptides to measure binding affinity, in contrast to the full-length proteins that serve as the naturally occurring ligands for PEX5. Furthermore, the assumption has been made that only the terminal three residues serve to define the PTS1. However, previous studies have suggested that residues upstream of the tripep-

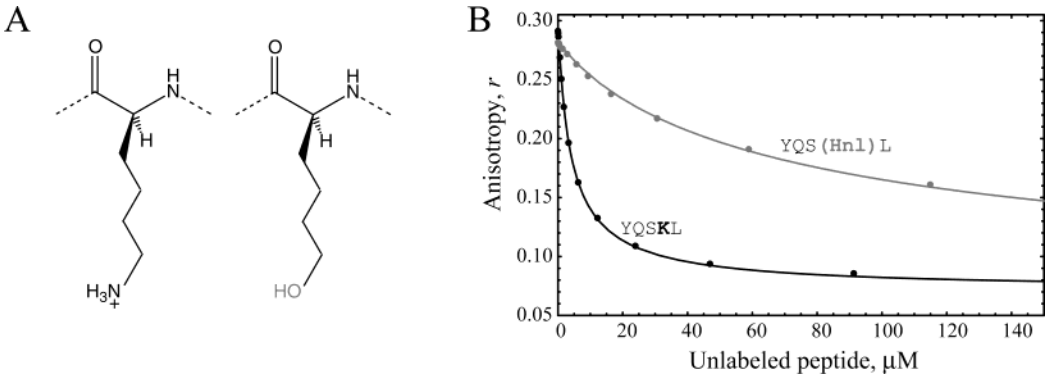

FIGURE 4: Replacement of lysine at position -2 with hydroxynorleucine (Hnl). (A) Comparison of the chemical structures of lysine (left) with 6-hydroxynorleucine (right). (B) Competition titrations and fitted curves of YQSKL (black) vs YQS(Hnl)L (gray).

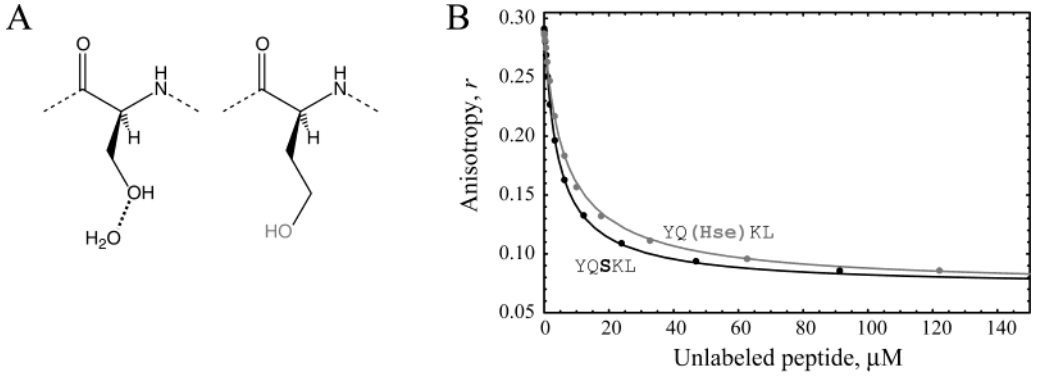

FIGURE 5: Replacement of serine at position -3 with homoserine (Hse). (A) Comparison of the chemical structures of serine bound to a water molecule (left) with homoserine (right). (B) Competition titrations and fitted curves of YQSKL (black) vs YQ(Hse)KL (gray).

tide targeting sequence may contribute to binding (*11*, *18*, *19*). It is possible that the identity of these upstream residues may enable an otherwise nonfunctional signal to cross the affinity threshold and allow peroxisomal import. Experiments with additional peptides are underway to explore this issue.

The thermodynamic profiles at positions -1, -2, and -3 that we have obtained are quite consistent with those anticipated from the crystal structure of the PEX5-C:PTS1 complex. The recognition pocket for position -1 is hydrophobic with considerable shape specificity resulting in nearly 2 orders of magnitude of discrimination between leucine and isoleucine. The specificity in position -2 appears to be largely determined by electrostatic effects. Peptides with both lysine and arginine bind with high affinity. Examination of the crystal structure reveals the distribution of fully charged side chains of PEX5-C relative to the nitrogen atom of the lysine side chain. Three glutamate residues, Glu 346, Glu 348, and Glu 379, are less than 7 Å from this atom while one lysine, Lys 520, which interacts primarily with the terminal carboxylate of the PTS1 peptide, is within 7 Å. Furthermore, 36 glutamate and aspartate residues are within 10−40 Å of the nitrogen atom, while only 22 lysine and arginine residues are in this range. Simple calculations, assuming a dielectric constant of 80, reveal a net electrostatic interaction of −3.9 kcal mol^{-1} between PEX5-C and the positive charge of the Lys (-2) side chain, with significant contributions from groups within 7 Å (−1.4 kcal mol^{-1}) and a net of −2.5 kcal mol^{-1} from the more distant groups. The use of lower dielectric constants would increase the magnitude of these calculated values.

These observations have particular relevance for three of the peptides studied. First, the peptide with 6-hydroxynorleucine in position -2 was used to directly probe these electrostatic effects. The observed discrimination between lysine and hydroxynorleucine is 1.9 kcal mol^{-1}, a value less than the calculated net electrostatic interaction between PEX5-C and the side chain ammonium of Lys (-2) determined above. However, this difference is anticipated by the energetic cost of partially desolvating this side chain, which is certainly higher for the charged lysine side chain than it is for 6-hydroxynorleucine. Second, the peptide with histidine in position -2 bound approximately 10-fold less tightly than YQSKL and more tightly than any peptide without a positively charged side chain. This suggests that the peptide binds with its imidazole ring protonated, and hence positively charged, despite the fact that these experiments were performed at pH 7.5 where the side chain is unlikely to be protonated free in solution. The energetic cost of protonating this side chain at pH 7.5, assuming a pK_a value of 6.0, is

$$\Delta G^\circ_{\text{protonation}} = -RT \ln(10^{(6.0-7.5)}) = 2.1 \text{ kcal mol}^{-1}$$

somewhat larger than the observed energy difference between the lysine- and histidine-containing peptides. This may be due to a difference in the true pK_a value for this residue. Alternatively, the histidine-containing peptide may be binding in both the protonated and the deprotonated forms; that is, the pK_a value of the histidine in the bound peptide may be close to 7.5.

Finally, the peptide with glutamate in position -2 binds very poorly to PEX5-C. If this peptide were to bind in its negatively charged form, the expected electrostatic penalty would be 3.9 kcal mol^{-1}, based on the analysis above. The cost of desolvating the negatively charged side chain would

be added to this value, yielding a calculated energy difference between YQSKL and YQSEL consistent with the observed value of >5 kcal mol^{-1}. Alternatively, the glutamate residue could be protonated, and hence, neutral at a cost of 4.8 kcal mol^{-1}, assuming a pK_a value of 4.0. Given the relatively modest binding of peptides with neutral side chains such as 6-hydroxynorleucine and asparagine, this protonation cost would also place the predicted $\Delta\Delta G°$ for the glutamic acid-containing peptide within the observed range.

It is clear from previous studies that the PTS1 variability profile is species-specific (*10*−*14*): sequences that do not function as signals in humans may be functional in other organisms. From an energetic standpoint, this observation could be the result of one or both of the following: (1) the receptors from different organisms are able to bind to these variant sequences tighter than human PEX5, bringing the affinities below threshold, or (2) the effective threshold affinity in these other species is raised such that weaker signals are now functional, a phenomenon that may be a reflection of species-specific differences in other factors within the import pathway. Further studies using this assay with PEX5 orthologs from other organisms may provide insight as to the nature of these differences. Of particular interest would be the species-specific changes in affinity for PEX5 from a group of parasites including *Trypanosoma brucei* (*20*), the causative organism for African sleeping sickness, and *Leishmania donovani* (*21*), the organism responsible for leishmaniasis. These parasites package their glycolytic enzymes in the glycosome (*22*), a relative of the peroxisome that also uses the PEX5:PTS1 system for proper protein targeting (*23*). Identification of sequences that would interfere with binding to the parasitic PEX5 but do not cross the functional threshold in humans would be valuable starting points for antiparasitic drug design.

ACKNOWLEDGMENT

We thank Dr. Howard Dintzis for helpful suggestions with the experimental design.

REFERENCES

1. van den Bosch, H., Schutgens, R. B. H., Wanders, R. J. A., and Tager, J. M. (1992) *Annu. Rev. Biochem. 61*, 157−97.
2. Gould, S. J., and Valle, D. (2000) *Trends Genet. 16*, 340−5.
3. Gould, S. J., Raymond, G. V., and Valle, D. (2001) in *The Metabolic and Molecular Bases of Inherited Disease* (Scriver, C. R., Beaudet, A. L., Sly, W. S., and Valle, D., Eds.) pp 3181−217, McGraw-Hill, New York.
4. Gould, S. J., Keller, G. A., Hosken, N., Wilkinson, J., and Subramani, S. (1989) *J. Cell Biol. 108*, 1657−64.
5. Dodt, G., Braverman, N., Wong, C., Moser, A., Moser, H. W., Watkins, P., Valle, D., and Gould, S. J. (1995) *Nat. Genet. 9*, 115−25.
6. Dodt, G., and Gould, S. J. (1996) *J. Cell Biol. 135*, 1763−74.
7. Terlecky, S. R., Nuttley, W. M., McCollum, D., Sock, E., and Subramani, S. (1995) *EMBO J. 14*, 3627−34.
8. Gatto, G. J., Jr., Geisbrecht, B. V., Gould, S. J., and Berg, J. M. (2000) *Nat. Struct. Biol. 7*, 1091−5.
9. Swinkels, B. W., Gould, S. J., and Subramani, S. (1992) *FEBS Lett. 305*, 133−6.
10. Elgersma, Y., Vos, A., van den Berg, M., van Roermund, C. W. T., van der Sluijs, P., Distel, B., and Tabak, H. F. (1996) *J. Biol. Chem. 271*, 26375−82.
11. Lametschwandtner, G., Brocard, C., Fransen, M., Van Veldhoven, P., Berger, J., and Hartig, A. (1998) *J. Biol. Chem. 273*, 33635−43.
12. Sommer, J. M., Cheng, Q.-L., Keller, G. A., and Wang, C. C. (1992) *Mol. Biol. Cell 3*, 749−59.
13. Mullen, R. T., Lee, M. S., Flynn, C. R., and Trelease, R. N. (1997) *Plant Physiol. 115*, 881−9.
14. Kragler, F., Lametschwandtner, G., Christmann, J., Hartig, A., and Harada, J. J. (1998) *Proc. Natl. Acad. Sci. U.S.A. 95*, 13336−41.
15. Godwin, H. A., and Berg, J. M. (1996) *J. Am. Chem. Soc. 118*, 6514−5.
16. Lakowicz, J. R. (1983) *Principles of Fluorescence Spectroscopy*, Plenum Press, New York.
17. Lundblad, J. R., Laurance, M., and Goodman, R. H. (1996) *Mol. Endocrinol. 10*, 607−12.
18. Purdue, P. E., and Lazarow, P. B. (1996) *J. Cell Biol. 134*, 849−62.
19. Amery, L., Brees, C., Baes, M., Setoyama, C., Miura, R., Mannaerts, G. P., and Van Veldhoven, P. P. (1998) *Biochem. J. 336*, 367−71.
20. de Walque, S., Kiel, J. A., Veenhuis, M., Opperdoes, F. R., and Michels, P. A. (1999) *Mol. Biochem. Parasitol. 104*, 106−19.
21. Jardim, A., Liu, W., Zheleznova, E., and Ullman, B. (2000) *J. Biol. Chem. 275*, 13637−44.
22. Opperdoes, F. R. (1987) *Annu. Rev. Microbiol. 41*, 127−51.
23. Keller, G. A., Krisans, S., Gould, S. J., Sommer, J. M., Wang, C. C., Schliebs, W., Kunau, W., Brody, S., and Subramani, S. (1991) *J. Cell Biol. 114*, 893−904.
24. Kraulis, P. J. (1991) *J. Appl. Crystallogr. 24*, 946−50.

BI027034Z